Supplementary Material for

Revisiting the applicability and constraints of molybdenum and uranium-based paleo redox proxies: comparing two contrasting sill fjords

K. Mareike Paul, Martijn Hermans, Sami A. Jokinen, Inda Brinkmann, Helena L. Filipsson, and Tom Jilbert

Table of contents

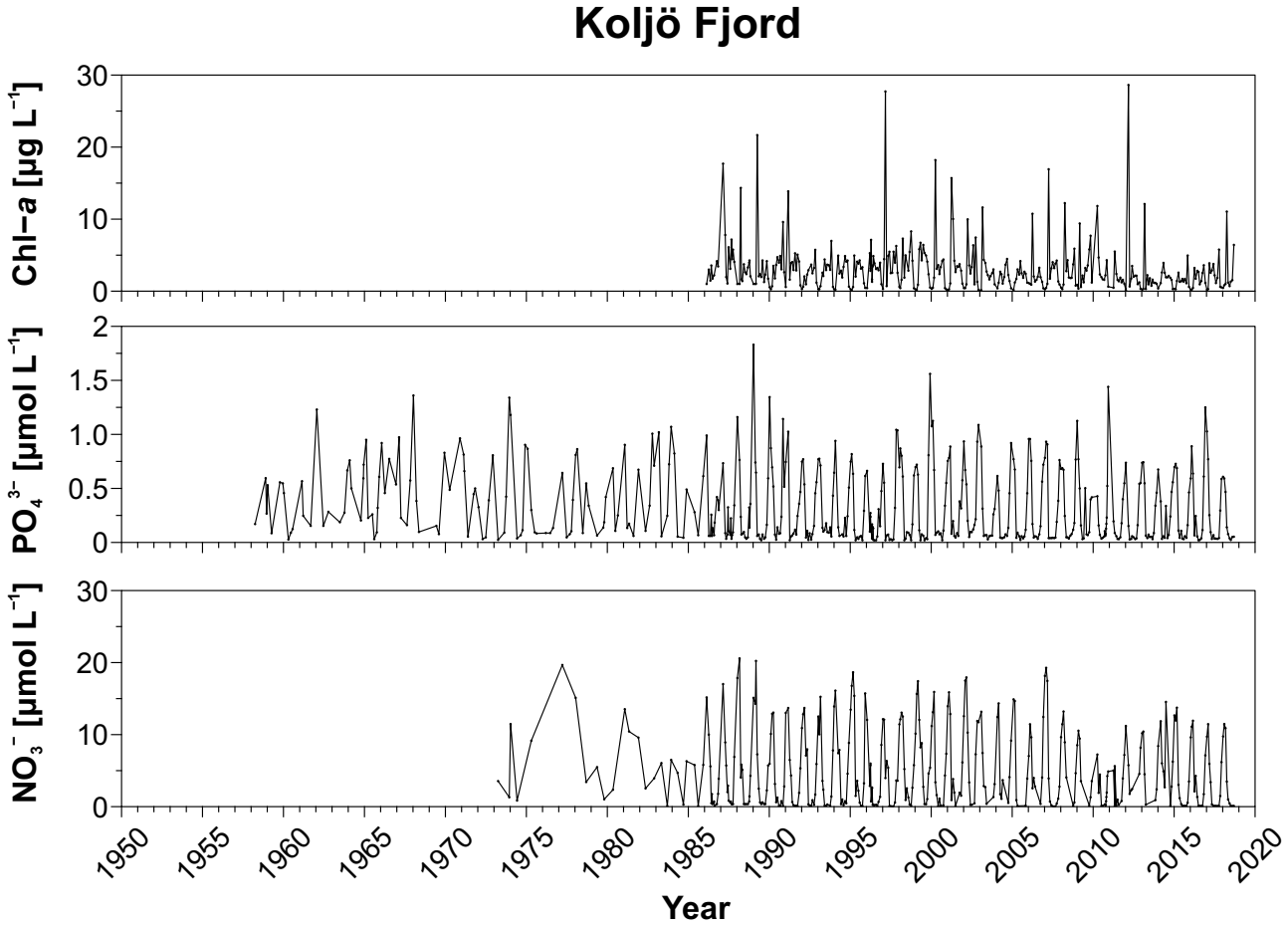

Figure S1. Bottom water nutrient (PO_4^{3-}+NO_3^-) and chlorophyll-*a* (average 0−10 m) monitoring data of for Koljö Fjord between 1950 and 2018 (SMHI, 2020).

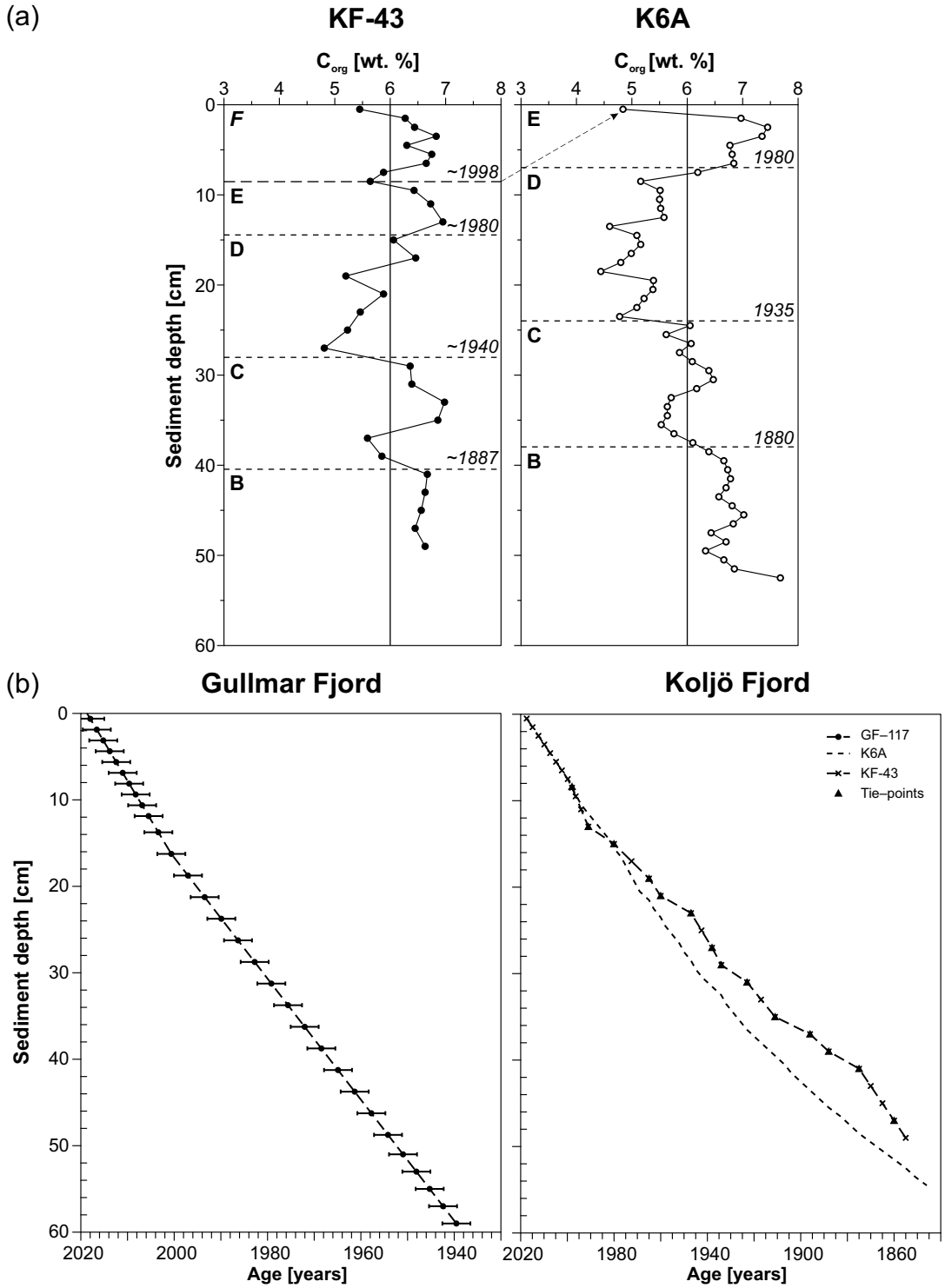

Figure S2. (a) C_{org} based age model of KF-43 (left panel) based on a previously dated sediment core K6A (right panel, Filipsson and Nordberg, 2004a) from the same sampling location at Koljö Fjord. The letters B-E refer to the units described Filipsson and Nordberg (2004a) based on the C_{org} content (6 wt. % threshold). Based on this approach, we added the unit *F*, which covers the period from 1998 (end of unit E, see dashed arrow) to 2018. (b) Left panel: age model for Gullmar Fjord (GF-117) based on average sedimentation rates estimated by ^{210}Pb and biostratigraphy (Nordberg et al., 2000; Filipsson and Nordberg, 2004b). Error bars, representing a margin of error of ±3 years for the ^{210}Pb ages, were added to the calculated ages (as per Roos, 1989 and Nordberg et al., 2000). Right panel: age model for Koljö Fjord (KF-43) based on tuning with the dated C_{org} (a) using QAnalySeries (Kotov and Paelike, 2018). The black triangles represent the 14 tie-points used for the tuning. The dashed line shows the original depth vs. age model for K6A, displaced by 8.5 cm downwards to account for sediment accumulation between 1998 (sampling year of K6A)–2018 (sampling year of KF-43, see text).

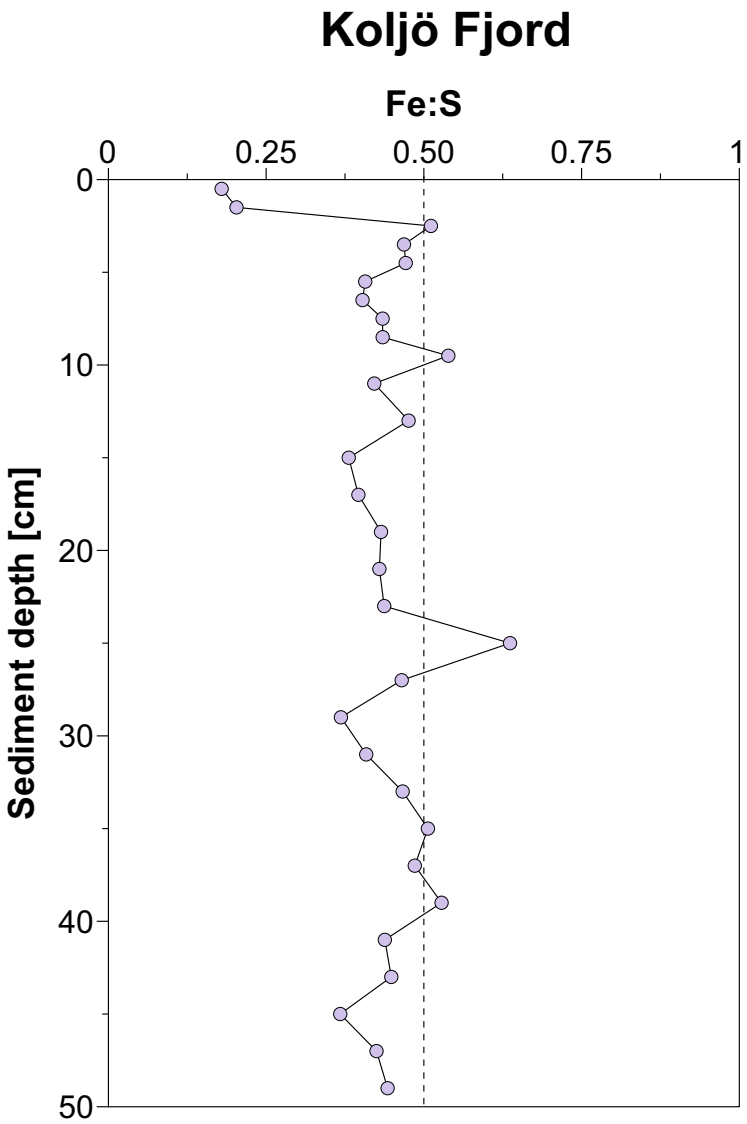

Figure S3. Fe:S ratio at Koljö Fjord based on Fe and S contents in fraction F5 from the extraction protocol (**Table 1** main text). The dashed line shows the 2:1 ratio, which is indicative for pyrite.

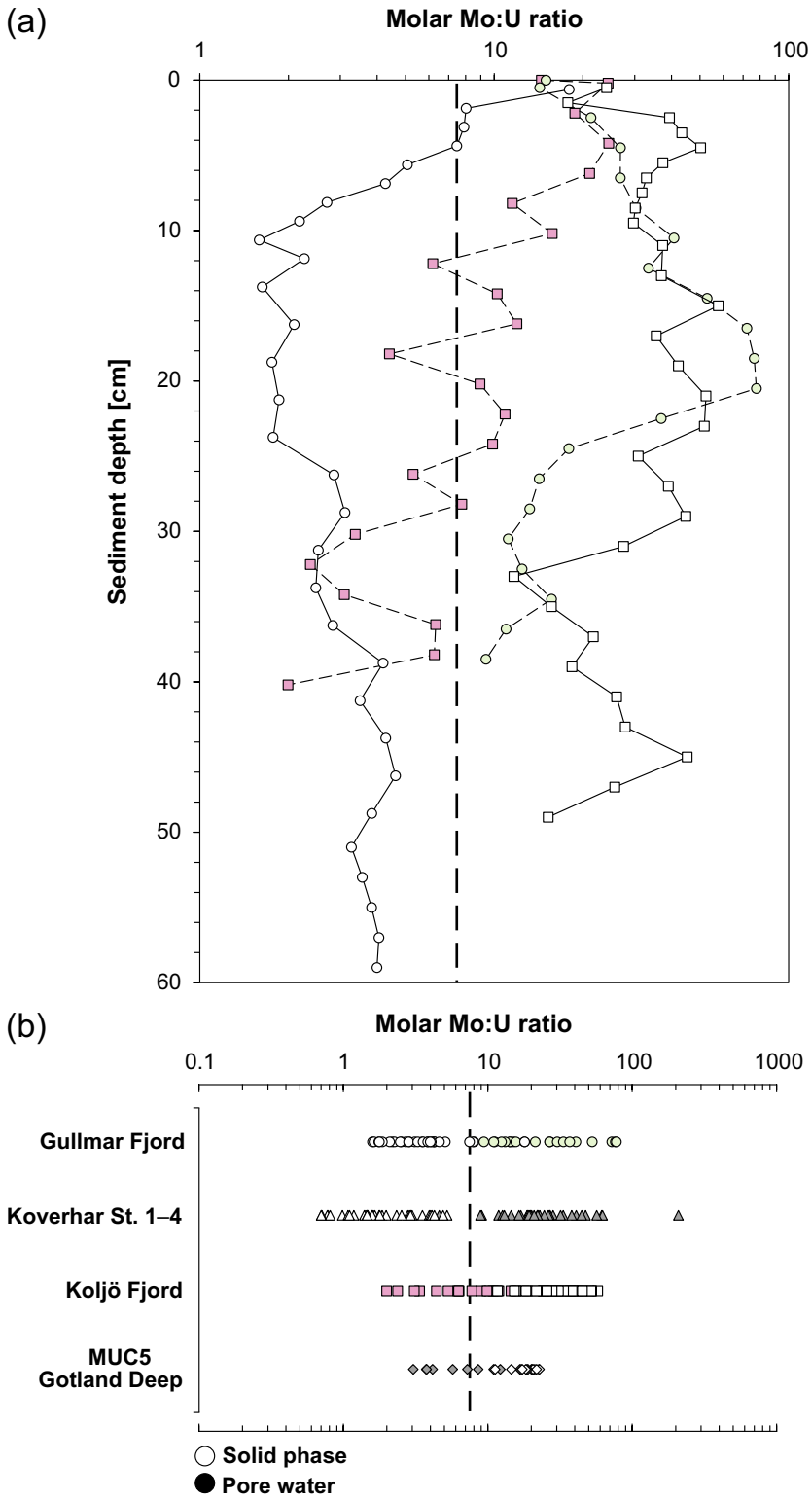

Figure S4. (a) Pore water (filled symbols) and solid phase (empty symbols) molar Mo:U ratio at Gullmar– and Koljö Fjord, (b) compared to literature data (Koverhar St. 1–4 was taken from Jokinen et al., 2020, and MUC5 from Scholz et al., 2013). In both panels, the Mo:U ratio is shown on $\log_{10}$ scale.

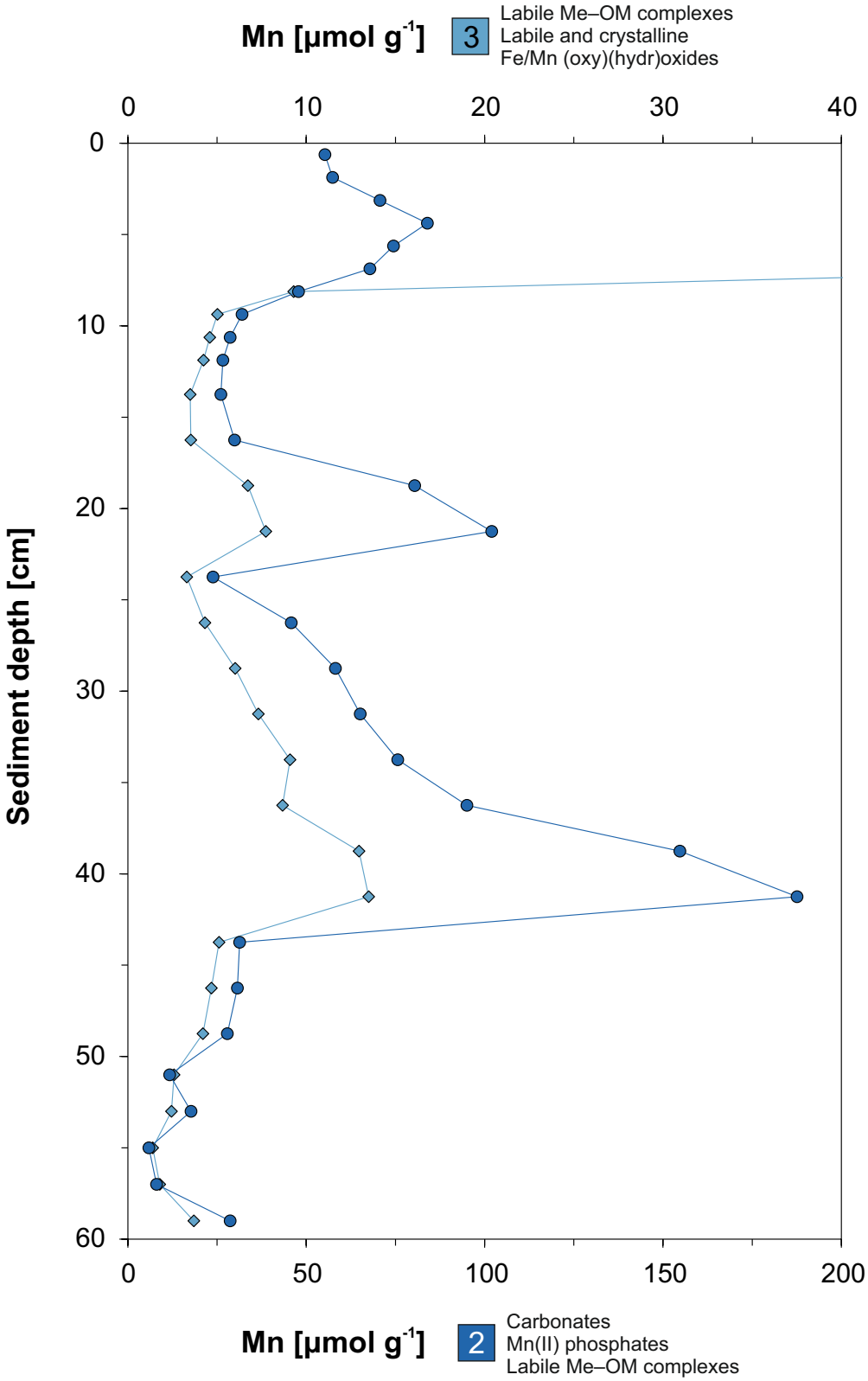

Figure S5. Sediment covariation between Mn F2 (dark blue circles, lower x-axis) and F3 (middle blue diamonds, lower x-axis) at Gullmar Fjord.

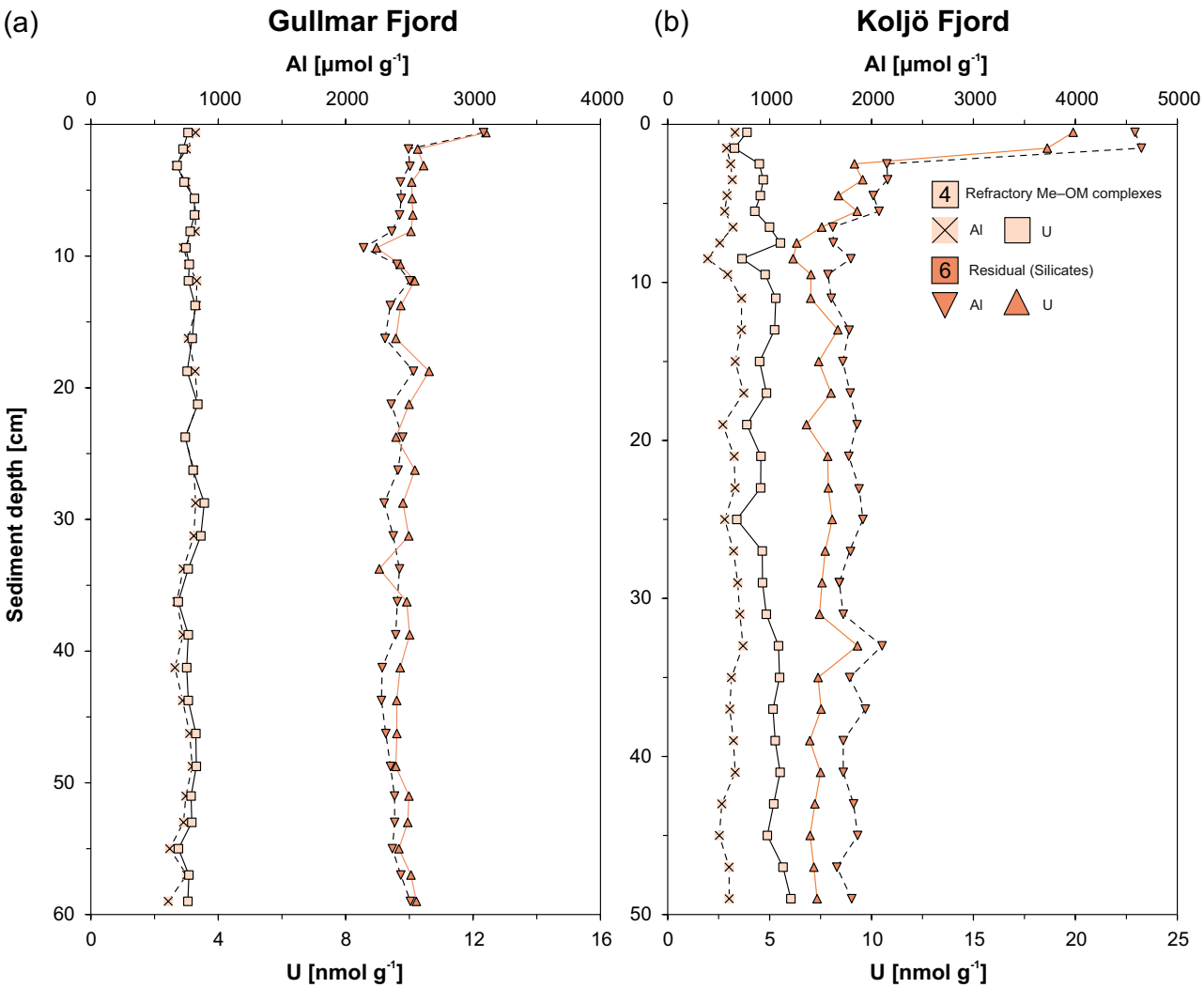

Figure S6. Sediment covariation between (a) U and Al in F4 and F6 at Gullmar– and (b) Koljö Fjord. Light orange filled squares represent U in F4, and light orange filled squares with a black cross show Al in F4. Orange filled triangles represent U in F6, inversed orange filled triangles show Al in F6.

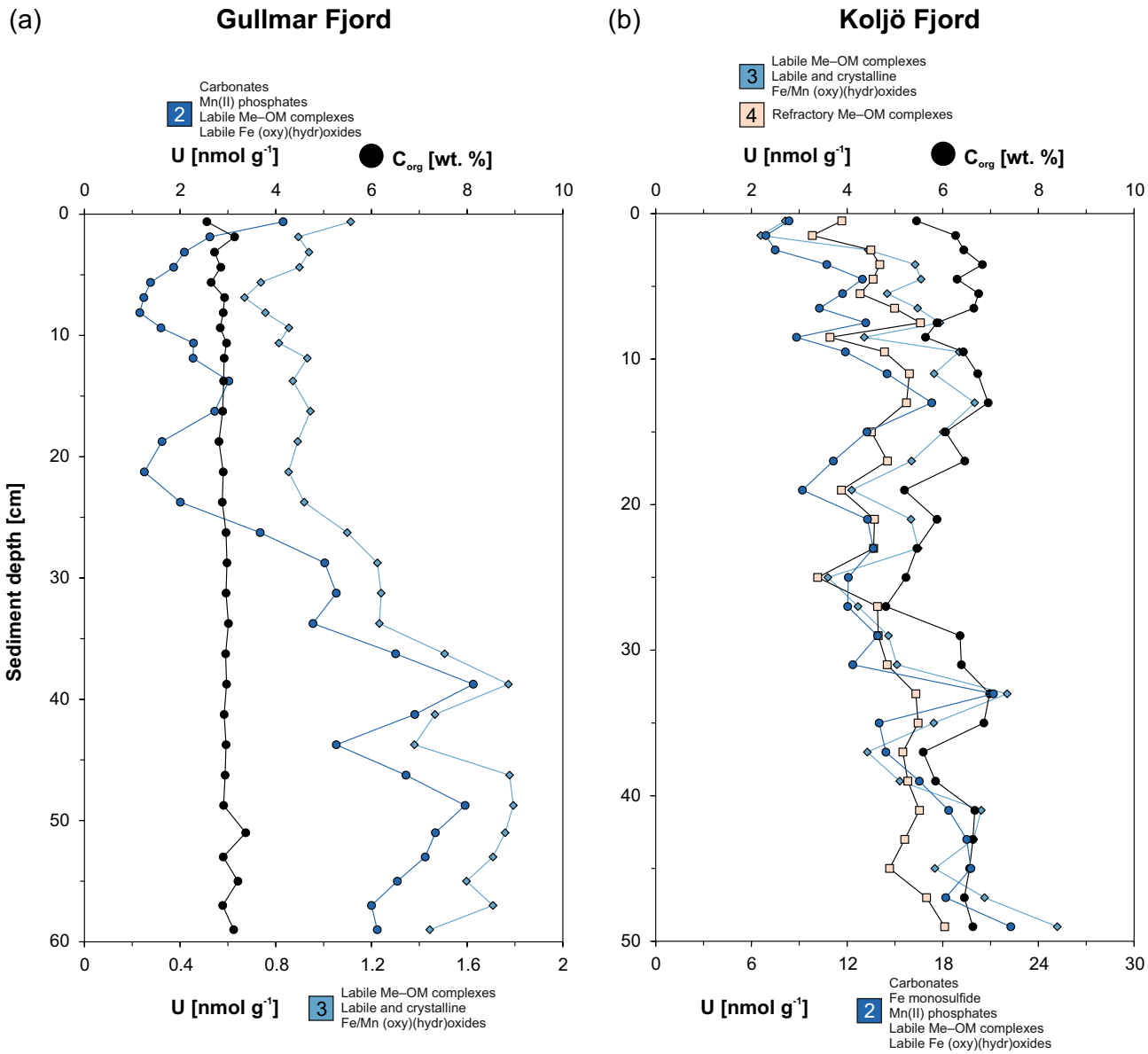

Figure S7. Sediment covariation between (a) C_{org} (black circles) and U in F2 (dark blue circles), F3 (middle blue diamonds), and F4 (light orange squares) at Gullmar – and (b) Koljö Fjord.

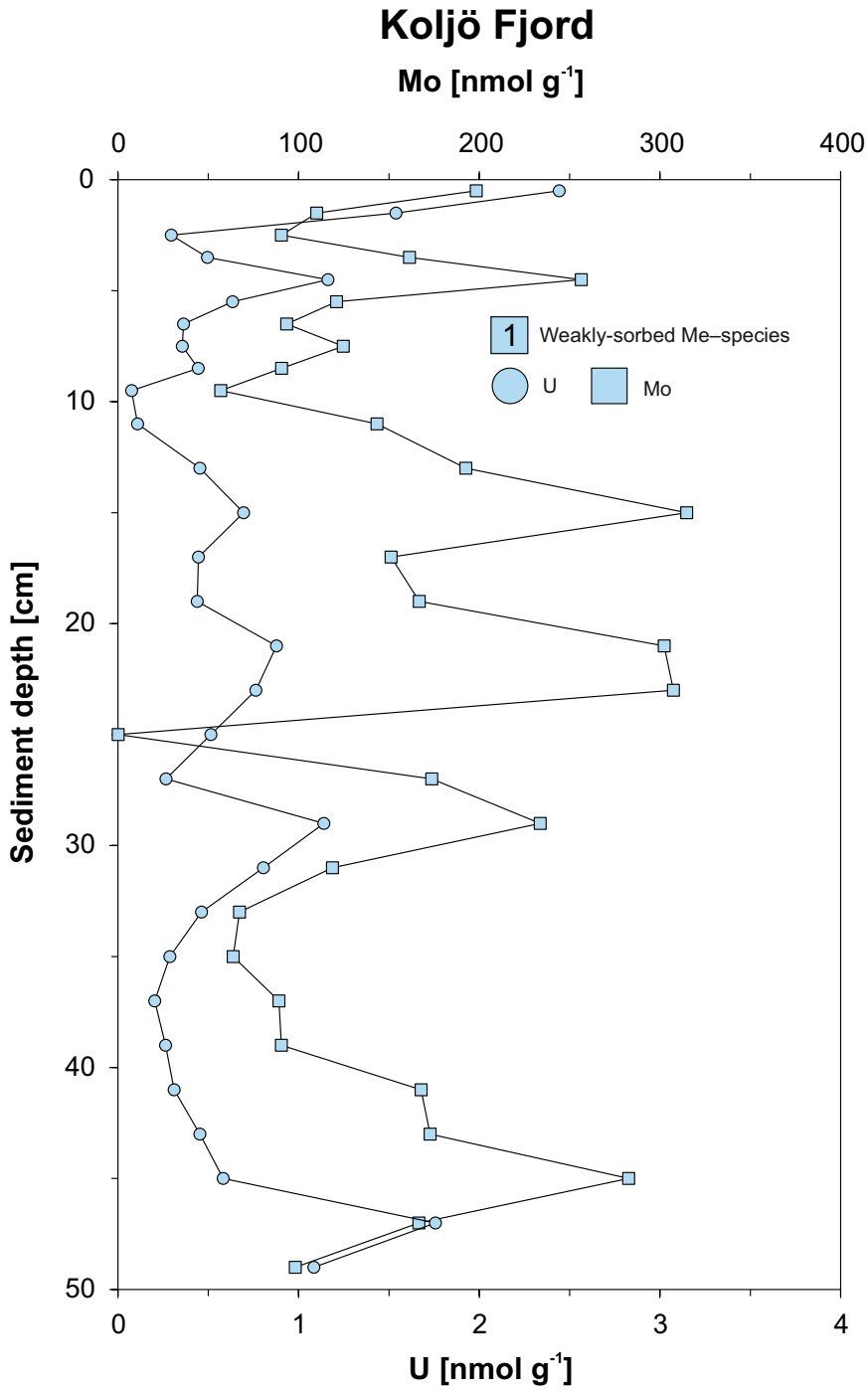

Figure S8. Sediment covariation between Mo (light blue squares, upper x-axis) and U (light blue circles, lower x-axis) in F1 at Koljö Fjord.

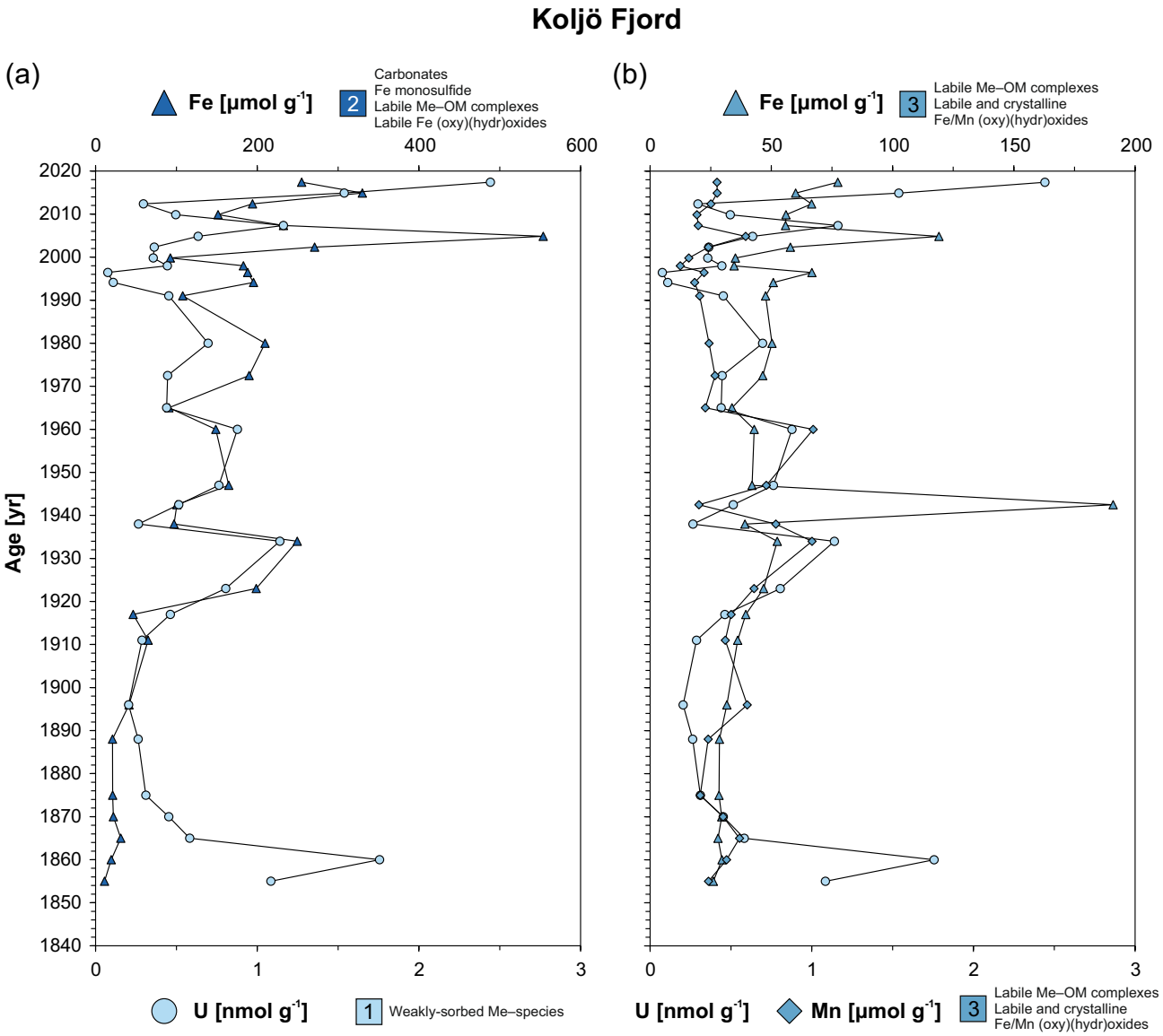

Figure S9. Covariation between (a) U in F1 (light blue circles, lower x-axis) with Fe in F2 (dark blue triangles), and (b) between U in F1 (light blue circles) with Mn (middle blue diamonds) and Fe (middle blue triangles) in F3 at Koljö Fjord.

References

Filipsson, H. L. and Nordberg, K.: A 200-year environmental record of a low-oxygen fjord, Sweden, elucidated by benthic foraminifera, sediment characteristics and hydrographic data, J. Foramin. Res., 34, 277-293, doi: 10.2113/34.4.277, 2004a.

Filipsson, H. L. and Nordberg, K.: Climate variations, an overlooked factor influencing the recent marine environment. An example from Gullmar Fjord, Sweden, illustrated by benthic foraminifera and hydrographic data, Estuaries, 27, 867-881, doi: 10.1007/Bf02912048, 2004b.

Jokinen, S. A., Koho, K., Virtasalo, J. J., and Jilbert, T.: Depth and intensity of the sulfate-methane transition zone control sedimentary molybdenum and uranium sequestration in a eutrophic low-salinity setting, Appl. Geochem., 122, doi: 10.1016/j.apgeochem.2020.104767, 2020.

Kotov, S. and Paelike, H.: QAnalySeries-a cross-platform time series tuning and analysis tool, AGU Fall Meeting Abstracts, PP53D-1230,

Nordberg, K., Gustafsson, M., and Krantz, A. L.: Decreasing oxygen concentrations in the Gullmar Fjord, Sweden, as confirmed by benthic foraminifera, and the possible association with NAO, J Marine Syst, 23, 303-316, doi: 10.1016/S0924-7963(99)00067-6, 2000.

Scholz, F., McManus, J., and Sommer, S.: The manganese and iron shuttle in a modern euxinic basin and implications for molybdenum cycling at euxinic ocean margins, Chem. Geol., 355, 56-68, doi: 10.1016/j.chemgeo.2013.07.006, 2013.

SMHI (2020) Water chemistry data 1950–2018. Svenskt HavsARKivs (SHARK) hydrdographic database Swedish Meteorological and Hydrological Institute (SMHI), https://sharkweb.smhi.se/hamta-data/, last accessed: 03 September 2022.